



Title	Chemical Synthesis of NICOL, A Coligand Secreted Protein Mediating Mammalian Male Reproductive Tract Trans-luminal Signaling
Author(s)	Nagahama, Kenta; Takei, Toshiki; Ito, Shun et al.
Citation	Chemistry – A European Journal. 2025, 31(47), p. e01588
Version Type	VoR
URL	https://hdl.handle.net/11094/102754
rights	This article is licensed under a Creative Commons Attribution-NonCommercial-NoDerivatives 4.0 International License.
Note	

The University of Osaka Institutional Knowledge Archive : OUKA

<https://ir.library.osaka-u.ac.jp/>

The University of Osaka

Chemical Synthesis of NICOL, A Coligand Secreted Protein Mediating Mammalian Male Reproductive Tract Trans-luminal Signaling

Kenta Nagahama,^[a] Toshiki Takei,^[a] Shun Ito,^[a] Toshifumi Takao,^[a] Hironobu Hojo,^{*,[a]} and Daiji Kiyozumi^{*,[b]}

Dedicated to the memory of Professor Luis Moroder

The NELL2-interacting cofactor for lumicrine signaling (NICOL) is a small protein which forms a complex with the neural epidermal growth factor-like like 2 (NELL2) and engaged in sperm maturation in the epididymis. At present, the recombinant expression of NICOL is not efficient, which limits the precise understanding of the structure and function of NICOL. In this study, we first suc-

ceeded in the chemical synthesis of NICOL with NELL2 binding affinity. The synthesized NICOL possesses correct SS bond pairing, and its secondary structure is indistinguishable from that of the recombinant protein, indicating that the synthetic NICOL will be useful for structural and functional analyses of lumicrine signaling.

1. Introduction

In mammals, the spermatozoa produced in the testis are morphologically complete but functionally immature; they need further functional maturation in the epididymis, a highly coiled epithelial duct constituting a part of the sperm transport route, for their full fertilizing ability.^[1–4] If the spermatozoa are not properly matured by the epididymis, they will not be able to acquire the cellular functions necessary for fertilization, eventually resulting in a significant decrease in the male reproductive ability.

Recent studies have revealed a signaling mechanism to regulate sperm maturation in the epididymis. Proteins secreted by the testis flow to the epididymis via the reproductive tract and bind to their receptors on the surface of the epididymal luminal epithelium to activate its sperm-maturing ability.^[5–7] This type of secretion signaling is called “lumicrine”.^[8] To date, two secreted proteins have been identified as ligands for lumicrine signal-

ing: that is, neural epidermal growth factor-like like 2 (NELL2) and NELL2-interacting cofactor for lumicrine signaling (NICOL).^[9] Mice lacking NELL2 or NICOL are male infertile because of improper functional maturation of their spermatozoa.^[7,9] NICOL is associated with NELL2 to form a molecular complex,^[9,10] implying the molecular basis of the NICOL action.

Recombinant protein expression systems using mammalian cell cultures have been widely employed to produce secreted proteins.^[7,9,10–19] For the preparation of lumicrine ligand proteins, mammalian transient expression systems have also been utilized.^[7,9,10] These systems are advantageous in supporting proper protein folding and the acquisition of post-translational modifications, including disulfide (SS) bond formation. However, proteins expressed in such systems often exhibit heterogeneity in folding and post-translational modifications, making it difficult to obtain structurally homogeneous proteins, which are essential for precise molecular functional analysis. In addition, structure–function correlation studies require the preparation of a substantial quantity of protein, but the high cost of culture media and transfection reagents, combined with the prolonged duration typically required for cell cultivation from gene transfection to protein purification, renders large-scale production using mammalian expression systems both time-consuming and economically inefficient.

In contrast to mammalian expression systems, chemical synthesis of polypeptides enables the precise design and incorporation of post-translational modifications and allows for controlled folding processes following synthesis. Although these procedures require additional steps, chemical synthesis offers several significant advantages, including a shorter preparation time, ease of scale-up, higher yields, and superior structural homogeneity. Moreover, it provides an exceptional flexibility for introducing artificial chemical modifications, making it a powerful approach for investigating protein functions at the molecular level. Solid-phase peptide synthesis (SPPS) is particularly suitable

[a] K. Nagahama, Dr. T. Takei, Dr. S. Ito, Prof. T. Takao, Prof. Dr. H. Hojo
Institute for Protein Research, The University of Osaka, 3-2 Yamadaoka,
Suita, Osaka 565-0871, Japan
E-mail: hojo@protein.osaka-u.ac.jp

[b] Dr. D. Kiyozumi
Research Organization of Science and Technology, Ritsumeikan University,
1-1, Noji-higashi, Kusatsu Shiga 525-8577, Japan
E-mail: kiyozumi@fc.ritsumei.ac.jp

Supporting information for this article is available on the WWW under
<https://doi.org/10.1002/chem.202501588>

© 2025 The Author(s). Chemistry – A European Journal published by Wiley-VCH GmbH. This is an open access article under the terms of the Creative Commons Attribution-NonCommercial-NoDerivs License, which permits use and distribution in any medium, provided the original work is properly cited, the use is non-commercial and no modifications or adaptations are made.

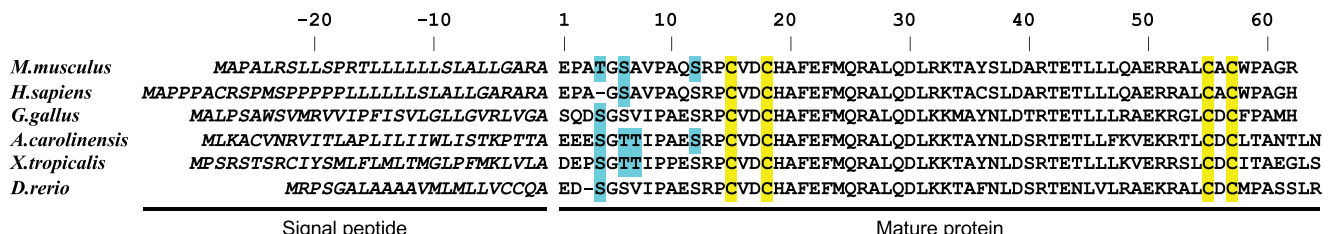


Figure 1. A sequence alignment of NICOL proteins of multiple species. UniProt entries of NICOL proteins are as follows: *M.musculus* (Q3UR78), *H.sapiens* (Q5BL8), *G.gallus* (E1BC3), *A.carolinensis* (H9GV37), *X.tropicalis* (A0A803J543), *D.rerio* (E7FEX9). Signal sequences are indicated in italics. Conserved Cys residues are highlighted with yellow. Potential O-glycosylation sites are highlighted with cyan.

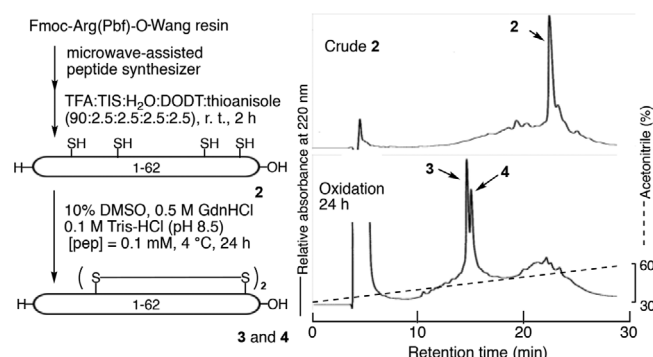


Figure 2. RPHPLC profile of the crude product 2 obtained by the SPPS and the ones 3 and 4 obtained after the oxidative folding reaction. Column: Cosmobil Protein R (4.6 x 250 mm), eluent: MeCN aq containing 0.1% TFA at the flow rate of 1.0 mL·min⁻¹.

for synthesizing polypeptides of up to approximately 60 amino acid residues.^[20] Given that mature NICOL proteins consist of 60–70 residues, they fall within or close to the upper limit of this synthetic range. In the present study, we chemically synthesized the mouse NICOL protein and investigated its molecular properties, with the aim of establishing a foundation for its structure-based functional analysis.

2. Results and Discussion

2.1. Synthesis of NICOL by the Random SS Bond Formation

The amino acid sequence of mouse NICOL is shown in Figure 1. Mouse NICOL has four cysteine residues, that is, Cys¹⁵, Cys¹⁸, Cys⁵⁵, and Cys⁵⁷. These cysteine residues are evolutionarily conserved among species, suggesting the presence of SS bonds, although the mode of their pairing is not known. In addition, the matrix-assisted laser desorption ionization time-of-flight (MALDI-TOF) mass spectrometry (MS) analysis of recombinant mouse NICOL 1 showed that it is heterogeneously glycosylated by O-glycan, which is composed of di- and monosialylated core 1 sugar (Figure S1). As the significance of the sugar chain on the biological activity of NICOL is not known at present, here, the nonglycosylated NICOL was synthesized and analyzed its function. We first performed the SPPS of NICOL by the random SS bond formation to obtain the most thermodynamically stable SS isomer and determine its SS bond pairing (Figure 2). To realize the synthesis, the triphenylmethyl (Trt) group was used for the protection

of the side chain thiol group of all the cysteine residues. The entire sequence was synthesized by a microwave-assisted peptide synthesizer. After deprotection, the obtained crude peptide 2 was dissolved in 6 M GdnHCl to completely unfold the structure and then diluted with tris(hydroxymethyl)aminomethane (Tris) buffer containing DMSO to perform the oxidative folding reaction. After an overnight reaction, the folding was almost complete as shown in Figure 2. Two peaks, corresponding to peptides 3 and 4, were isolated by the reversed-phase high-performance liquid chromatography (RPHPLC) purification. The yield of 3 was 2.7% and for peak 4, it was 1.5%.

2.2. Determination of SS Bond Pairing of the Synthetic NICOL

The mode of the SS bonds of peptide 3 was determined as shown in Figure 3(a), following the reported procedure.^[21,22] The SS bond was partially reduced by the treatment with tris(2-carboxyethyl)phosphine (TCEP) under an acidic condition (pH 3.0) to avoid the shuffling of the SS bond. After 1 hour, 1-cyano-4-dimethylaminopyridinium tetrafluoroborate (CDAP) was added to cyanlate the free thiol groups. By this reaction, we could successfully obtain the NICOL having the two thiocyanate groups with one SS bond 5 (Figure 3(b)). After isolation of the product 5 by RPHPLC, it was treated with ammonia aq to cleave the peptide bond at the N-terminus of the cyanlated Cys. We could observe two main peaks on the HPLC profile as shown in Figure 3(b): a peak at around 20 minutes was identified as peptide 6, the other peak at around 50 minutes was peptide 7. These data support the SS bond pairing between Cys¹⁵ and Cys⁵⁵, and between Cys¹⁸ and Cys⁵⁷. In a similar manner, the same reaction was performed with peptide 4. The results support that the SS bond pairing between Cys¹⁵ and Cys⁵⁷, and between Cys¹⁸ and Cys⁵⁵ (Figure S2).

We then attempted the determination of the SS bond pairing of the recombinant mouse NICOL following the same procedure (Figure S3). The obtained fragments by the reaction were analyzed by an MS analysis. Due to the limited amount and heterogeneous glycosylation of the recombinant NICOL, we could not detect all of the expected mass values. However, the MALDI-TOF MS detection of the 1–17 fragment with free cysteine 12 and the 57–62 fragment with the N-terminal iminothiazolidine 13 after complete reduction of the ammonia-cleavage mixture suggests that the SS bond pairing is Cys¹⁵-Cys⁵⁵ and Cys¹⁸-Cys⁵⁷ (Figure S3), which corresponds to synthetic peptide 3.

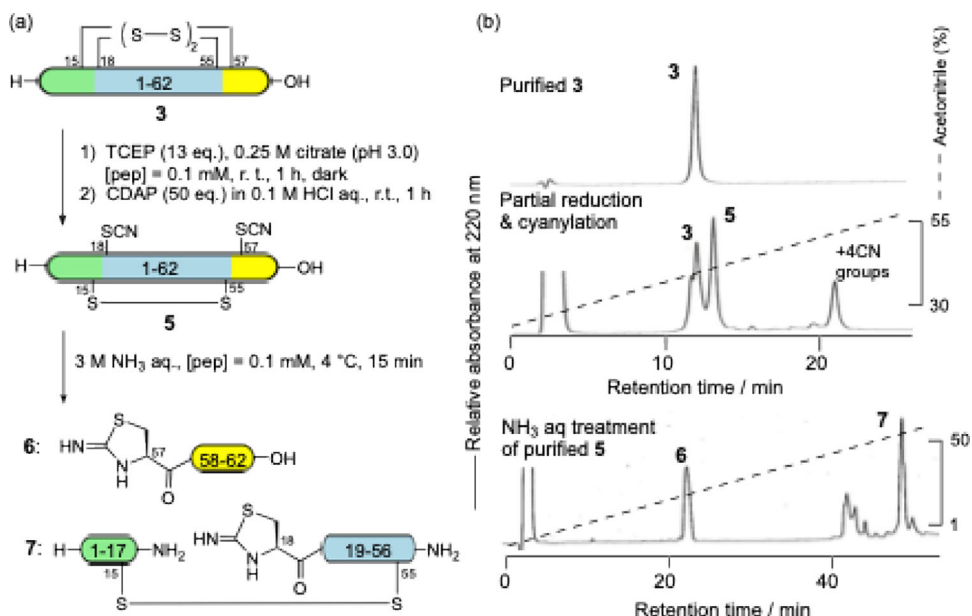


Figure 3. SS bond determination procedure of peptide 3 a) and the RPHPLC profile of the reaction b). Column: Mightysil RP-18 GP II (4.6 x 150 mm), eluent: MeCN aq containing 0.1% TFA at the flow rate of 1.0 mL·min⁻¹.

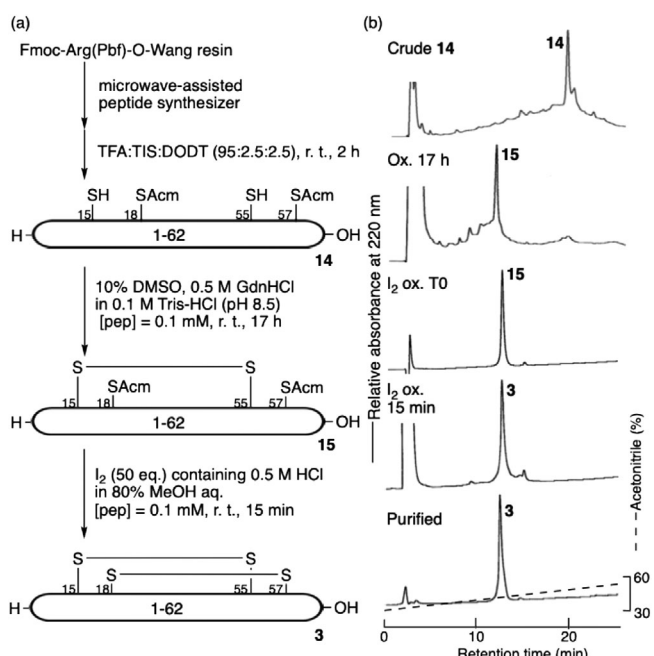


Figure 4. Synthetic procedure for NICOL 3 by the selective SS bond formation a) and the results of the synthesis b). The elution conditions are the same as those in Figure 3.

2.3. Synthesis of NICOL with the Native SS Pairing

To obtain a sufficient amount of NICOL with the native SS pairing for structural and functional analyses, the resynthesis was performed using the stepwise selective SS bond formation following the scheme in Figure 4. For the thiol protecting group of Cys¹⁵ and Cys⁵⁵, the Trt group was used, and for Cys¹⁸ and Cys⁵⁷, the acetamidomethyl (Acm) group was used, then the SPPS was performed. After deprotection, the crude peptide 14 was subjected

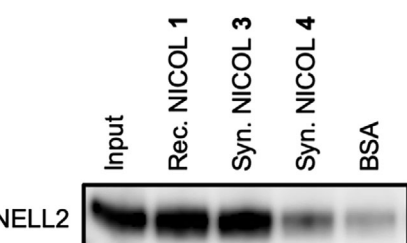


Figure 5. NELL2 pulldown assay using recombinant and synthetic NICOL. Immunoblot analysis of NELL2 pulled down with recombinant NICOL 1, two synthetic NICOL 3 and 4, and BSA (negative control). Input NELL2 protein was also included as a reference. The uncropped image is shown in Figure S15.

to the oxidative folding reaction using DMSO as an oxidant to form the SS bond between Cys¹⁵ and Cys⁵⁵, which was confirmed by an MS analysis. The second SS bond was formed by I₂ oxidation of the Acm-protected Cys residues. The reaction efficiently proceeded to give the desired NICOL with the native SS pairings 3 in a yield of 3.4%. The product was confirmed by an MS analysis and amino acid composition analysis.

2.4. NICOL-NELL2 Interaction Assay

The binding of the synthetic NICOL to NELL2 was examined using an in vitro pull-down assay. The synthetic NICOL proteins were immobilized on NHS-activated agarose beads and incubated with a solution containing purified NELL2 to assess the binding interactions. As shown in Figure 5, compared with BSA, a negative control protein, the recombinant NICOL 1 exhibited stronger binding to NELL2. The synthetic NICOL with the native SS bond pairing 3 also exhibited a binding activity, whereas the synthetic NICOL with the SS isomer 4 showed a

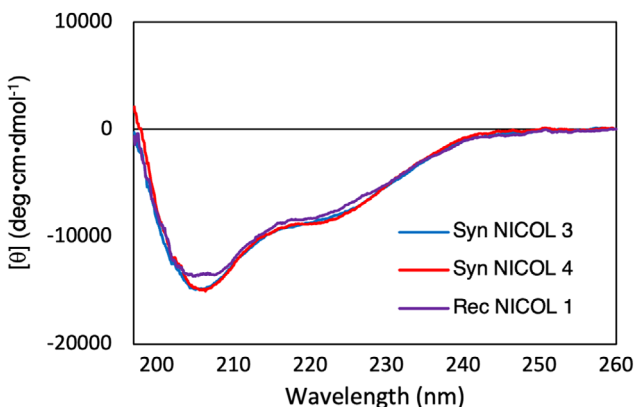


Figure 6. CD spectrum of NICOLs measured in MES buffer (pH 6.0).

reduced NELL2 binding, indicating that the correct SS bond formation contributes to NELL2 binding activity in synthetic NICOL. It is to be noted that in this pull-down assay, NICOL peptides were immobilized rather than NELL2. This approach was chosen because it allows simultaneous comparison of multiple NICOL-derived peptides. As the pulled-down components—recombinant NICOL, synthetic peptides, and BSA—cannot be detected by the immunoblot with equal sensitivity under a NELL2-immobilized setup. Additionally, this design is consistent with our previous study,^[9] allowing direct comparison of results.

2.5. Characterization of NICOL by CD Spectrum Measurement

The CD spectrum of the synthetic and recombinant NICOL was measured. As shown in Figure 6, all the NICOLs retained a very similar CD spectrum, indicating that the structures are quite similar, even that of the SS bond isomer 4.

2.6. The Binding of Synthetic NICOL with Recombinant NELL2 Using Surface Plasmon Resonance

The binding affinity of the synthetic NICOL to NELL2 was measured using surface plasmon resonance (SPR) spectroscopy. The recombinant mouse NELL2 having His₆ at its C-terminus was immobilized onto a sensor chip having nickel nitrilotriacetic acid (Ni-NTA) as a ligand using the NTA reagent kit (Cytiva). The synthetic mouse NICOL protein dissolved in running buffer was loaded as the analyte, and its association and dissociation kinetics were monitored using Biacore 8K (Cytiva). The rate and binding constant of the synthetic NICOL are summarized in Table 1. The synthetic NICOL with the native SS pairing 3 retained the higher association and lower dissociation rate constant, giving the lower K_D compared to the SS isomer 4, indicating that the native-type SS bond pairing contributes to fine interaction of NICOL with NELL2.

The parameters of peptides 3 and 4 do not appear to align with the pull-down results shown in Figure 5, as the difference in K_D values between native peptide 3 and isomer 4 primarily stems from their differing k_a values. In addition to

Table 1. Kinetic parameters of synthetic NICOLs for binding to recombinant NELL2 determined by SPR spectroscopy.

	Synthetic NICOL 3 [n = 21]	Synthetic NICOL 4 [n = 21]	Rec NICOL ^[a]
k_a ($10^4 \times 1/\text{Ms}$)	2.35 ± 0.27	1.38 ± 0.13	7.2
k_d ($10^{-4} \times 1/\text{s}$)	13.4 ± 1.3	15.7 ± 2.5	62
K_D (nM)	61.7 ± 4.4	145 ± 33	87

^[a] For recombinant NICOL, data was taken from ref. 9 and not determined by this study.

the distinct immobilization strategies employed (NELL2 immobilized in SPR vs. NICOL in the pull-down assay), the differing buffer conditions likely contributed to the observed discrepancies in binding behavior between the two assays. In the SPR experiments, we used PBS containing 0.05% (v/v) Tween® 20, which enables quantitative and real-time analysis of interaction kinetics. In contrast, the pull-down assay was conducted in TBS supplemented with 1% Triton X-100 and 1% BSA. This buffer, which includes both a detergent and a protein stabilizer, more closely mimics the complex environment of biological systems. Consequently, the pull-down assay is considered an endpoint-based and semi-quantitative method.

Compared with the previously reported k_a and k_d values of recombinant mouse NICOL,^[9] the synthetic NICOL 3 exhibited slower association and dissociation rates, indicating that recombinant NICOL interacts with NELL2 more dynamically. This difference may reflect structural variations beyond the peptide backbone and disulfide bonds, including the presence of glycosylation in recombinant NICOL. Such glycosylation may modulate the association and dissociation kinetics, potentially enabling cells to rapidly respond to changes in ligand availability. Further studies using glycosylated synthetic NICOL will be necessary to clarify the role of glycosylation in the NICOL–NELL2 interaction.

3. Conclusion

The SS bond pairing of the recombinant mouse NICOL was attempted by partial reduction, cyanylation, followed by ammonolysis. The results suggested that the SS pairings are Cys15–Cys55 and Cys18–Cys57. The random SS bond formation of the chemically synthesized NICOL shows that NICOL with the native SS bond pairing 3 is formed as a major product and is more hydrophilic, which rationalizes the correctness of the pairing. By using different thiol protecting groups, the stepwise selective SS bond formation was achieved to obtain NICOL with the correct SS bond. This realized the efficient synthesis of the NICOL with the native SS pairings for structural and functional analyses. The availability of the structurally-defined NICOL protein opens the way for further in-depth investigations. Future studies will focus on clarifying the role of NICOL glycosylation in lumicrine signaling and determining the crystal structure of NICOL for a full characterization of the NICOL–NELL2 interaction.

These efforts are expected to provide critical insights into the lumicrine signaling mechanism and facilitate the rational design of molecular probes or inhibitors targeting this pathway.

4. Materials and Methods

4.1. Recombinant Protein Expression and Purification

Recombinant mouse NICOL and NELL2 proteins were transiently expressed in 293-F cells (Invitrogen, #R79007) as described previously.^[7,9,10] Briefly, C-terminally 6xHis-tagged mouse NELL2 or C-terminally 8xHis-tagged mouse NICOL was transiently expressed in 293F cells according to the manufacturer's instruction and purified from the conditioned medium by affinity chromatography with Ni-NTA (Qiagen, #30210).

4.2. General Procedure for Peptide Synthesis

RPHPLC was carried out on Cosmosil Protein R (4.6×250 mm) (Nacalai Tesque Inc., Kyoto) or Mightysil RP-18 GP II (4.6×150 mm) (Kanto Chemical Co., Inc., Tokyo) using a linear increasing gradient of MeCN containing 0.1% TFA in 0.1% TFA/H₂O. Detection was done by an absorbance measurement at 220 nm. Electrospray ionization (ESI) MS was done using LCQ DECA XP Plus (Thermo Fisher Scientific, MA) or LCQ Fleet (Thermo Fisher Scientific, MA). MALDI-TOF MS was done with an autoflex (Bruker, MA) using α -cyano-4-hydroxycinnamic acid as a matrix. The amino acid composition of a peptide was determined using a LaChrom amino acid analyzer (Hitachi, Tokyo) after hydrolysis with 6 M HCl at 180 °C for 20 minutes in an evacuated sealed tube. SPPS was performed using a Liberty Blue microwave peptide synthesizer (CEM corporation, NC).

4.3. Synthesis of NICOL

4.3.1. Synthesis by Random SS Bond Formation

Starting from the Fmoc-Arg(Pbf)-Wang resin LL (360 mg, 0.10 mmol), the peptide chain was elongated by a microwave-assisted peptide synthesizer. The resultant resin was washed with DCM, followed by ether and dried *in vacuo* to yield H-Glu(OBu^t)-Pro-Ala-Thr(Bu^t)-Gly-Ser(Bu^t)-Ala-Val-Pro-Ala-Gln(Trt)-Ser(Bu^t)-Arg(Pbf)-Pro-Cys(Trt)-Val-Asp(OBu^t)-Cys(Trt)-His(Trt)-Ala-Phe-Glu(OBu^t)-Phe-Met-Gln(Trt)-Arg(Pbf)-Ala-Leu-Gln(Trt)-Asp(OBu^t)-Leu-Arg(Pbf)-Lys(Boc)-Thr(Bu^t)-Ala-Tyr(Bu^t)-Ser(Bu^t)-Leu-Asp(OBu^t)-Ala-Arg(Pbf)-Thr(Bu^t)-Glu(OBu^t)-Thr(Bu^t)-Leu-Leu-Leu-Gln(Trt)-Ala-Glu(OBu^t)-Arg(Pbf)-Arg(Pbf)-Ala-Leu-Cys(Trt)-Ala-Cys(Trt)-Trp(Boc)-Pro-Ala-Gly-Arg(Pbf)-Wang resin (1.2 g). The resin (1.2 g, 0.10 mmol) was treated with the TFA cocktail (TFA-triisopropylsilane (TIS)-H₂O-thioanisole-3,6-dioxa-1,8-octanedithiol (DODT), 90:2.5:2.5:2.5, 12 mL) for 2 hours at room temperature. The reaction mixture was filtered, and the filtrate was concentrated by an N₂ stream and precipitated with ether. The precipitate, peptide 2, was washed with ether

($\times 5$) and dried *in vacuo*. The crude peptide 2 was dissolved in 6.0 M GdnHCl aq. (100 mL) at 4 °C and diluted with 50 mM Tris containing 0.50 M GdnHCl and 10% DMSO (900 mL, pH 8.5). The resultant solution was stirred for 24 hours at 4 °C. The mixture was then acidified by the addition of 10% TFA aq. and filtered through omnipore 0.30 μ m PTFE membrane. The filtrate was purified by RPHPLC to isolate the two main peaks. Peptide 3: ESI MS, found: *m/z* 1719.6, 1376.1, 1147.1, calcd for [M+4H]⁴⁺: 1720.0, [M+5H]⁵⁺: 1376.2, [M+6H]⁶⁺: 1147.0. Amino acid analysis: Asp_{2.85(3)} Thr_{3.30(4)} Ser_{2.28(3)} Glu_{7.63(8)} Pro_{5.31(4)} Gly_{1.96(2)} Ala_{10.9(11)} Val_{1.87(2)} Met_{0.81(1)} Leu₇₍₇₎ Tyr_{0.58(1)} Phe_{1.78(2)} His_{0.94(1)} Arg_{6.70(7)}. Yield: 2.7% (18 mg, 2.7 μ mol). Peptide 4: ESI MS, found: *m/z* 1719.9, 1376.1, 1146.9, calcd for [M+4H]⁴⁺: 1720.0, [M+5H]⁵⁺: 1376.2, [M+6H]⁶⁺: 1147.0. Amino acid analysis: Asp_{2.87(3)} Thr_{3.31(4)} Ser_{2.21(3)} Glu_{7.50(8)} Pro_{8.96(4)} Gly_{1.65(2)} Ala_{11.0(11)} Val_{1.85(2)} Met_{0.43(1)} Leu₇₍₇₎ Tyr_{0.56(1)} Phe_{1.87(2)} His_{0.88(1)} Arg_{6.60(7)}. Yield: 1.5% (10 mg, 1.5 μ mol).

4.3.2. Determination of the SS Bond Pairing of NICOLs

Peptide 3: Peptide 3 (0.69 mg, 100 nmol) was dissolved in 0.25 M citrate (pH 3.0, 1.0 mL), then 0.10 M TCEP aq. (13 μ L) was added to the solution. The mixture was stored for 1 hour at room temperature under a dark condition. 0.50 M CDAP (1-cyano-4-dimethylamino-pyridinium tetrafluoroborate) in 0.10 M HCl aq. (98 μ L) was added to the solution, and the mixture was stirred for 1 hour at room temperature. The reaction was quenched by the addition of cysteamine hydrochloride aq. and purified by RPHPLC to give the partially reduced and cyanlated peptide 5. Peptide 5: ESI MS, found: *m/z* 1732.4, 1386.5, 1155.7, calcd for [M+4H]⁴⁺: 1733.0, [M+5H]⁵⁺: 1386.6, [M+6H]⁶⁺: 1155.6. Amino acid analysis: Asp_{3.52(3)} Thr_{3.52(4)} Ser_{2.84(3)} Glu_{8.20(8)} Pro_{4.50(4)} Gly_{3.10(2)} Ala_{13.4(11)} Val_{2.28(2)} Met_{0.82(1)} Leu₇₍₇₎ Tyr_{1.02(1)} Phe_{2.11(2)} His_{1.06(1)} Arg_{7.22(7)}. The peptide 5 (55 μ g, 8.0 nmol) was dissolved in 3.0 M NH₃ aq. (80 μ L) at 4 °C. The mixture was stirred for 15 minutes and acidified by the addition of 10% TFA aq. The mixture was analyzed by HPLC and ESI MS. Two peaks were isolated, which correspond to peptides 6 and 7. Peptide 6: ESI MS, found: *m/z* 714.4, calcd for [M+H]⁺: 714.3. Peptide 7: ESI MS, found: *m/z* 1563.3, 1250.7, 1042.3, calcd for [M+4H]⁴⁺: 1562.8, [M+5H]⁵⁺: 1250.4, [M+6H]⁶⁺: 1042.2.

Peptide 4: Peptide 4 (0.69 mg, 100 nmol) was treated by the same procedure as described for the preparation of peptide 5 to give the partially reduced and cyanlated peptide 8 (Figure S2). Peptide 8: ESI MS, found: *m/z* 1732.5, 1386.4, calcd for [M+4H]⁴⁺: 1733.0, [M+5H]⁵⁺: 1386.6. Amino acid analysis: Asp_{2.80(3)} Thr_{3.21(4)} Ser_{2.21(3)} Glu_{6.95(8)} Pro_{4.37(4)} Ala_{13.5(11)} Val_{1.88(2)} Met_{0.21(1)} Leu₇₍₇₎ Tyr_{0.56(1)} Phe_{1.84(2)} His_{0.90(1)} Arg_{6.47(7)}. Peptide 8 (0.072 mg, 10 nmol) was cleaved following the same procedure as previously described. The mixture was analyzed by HPLC and the three peaks corresponding to peptides 6, 9, and 10 were isolated. Peptide 6: ESI MS, found: *m/z* 714.5, calcd for [M+H]⁺: 714.3. Peptide 9: ESI MS, found: *m/z* 1366.9, 683.9 calcd for [M+H]⁺: 1366.7, [M+2H]²⁺: 683.9. Peptide 10: ESI MS, found: *m/z* 1627.9, 1221.3, 977.1 calcd for [M+3H]³⁺: 1627.5, [M+4H]⁴⁺: 1220.9, [M+5H]⁵⁺: 976.9.

Recombinant mouse NICOL 1: The recombinant mouse NICOL 1 (69 µg, 10 nmol) was dissolved in 0.25 M citrate (pH 3.0, 100 µL), then 0.10 M TCEP aq. (1.3 µL) was added to the solution. The mixture was stored for 20 minutes at room temperature under a dark condition. 0.50 M CDAP in 0.10 M HCl aq. (9.8 µL) was added to the solution and the mixture was stirred for 10 minutes at room temperature. The reaction was quenched by the addition of cysteamine hydrochloride aq. and purified by RP-HPLC to give the partially reduced and cyanated peptide 11. Peptide 11: ESI MS, tetrasaccharide NICOL found: *m/z* 1282.6, 1122.8, 998.3, calcd for [M+7H]⁷⁺: 1282.7, [M+8H]⁸⁺: 1122.5, [M+9H]⁹⁺: 997.9, trisaccharide NICOL found: *m/z* 1241.0, calcd for [M+7H]⁷⁺: 1241.1. The purified peptide 11 was dissolved in 3.0 M NH₃ aq. containing 10 mM TCEP (100 µL) at 4 °C. The mixture was stirred for 15 minutes and acidified by the addition of 10% TFA aq. The mixture was analyzed by HPLC and MALDI-TOF MS. Eluents were collected at 2-minute intervals, and in the fraction collected between 20.5 and 22.5 minutes, two peaks corresponding to peptides 12 and 13 were observed. Peptide 12: MALDI-TOF MS, found: *m/z* 1811.9, calcd for [M+H]⁺: 1812.0. Peptide 13: MALDI-TOF MS, found: *m/z* 1685.0, calcd for [M+H]⁺: 1685.8.

4.3.3. Synthesis of NICOL with the Native SS Bond Pairing by Selective SS Bond Formation

[Cys(Acm)^{18,57}]NICOL 15: Starting from the Fmoc-Arg(Pbf)-Wang resin LL (36 mg, 10 µmol), the peptide chain was elongated by a microwave-assisted peptide synthesizer. The resultant resin was washed with DCM followed by ether and dried *in vacuo* to yield H-Glu(OBu^t)-Pro-Ala-Thr(Bu^t)-Gly-Ser(Bu^t)-Ala-Val-Pro-Ala-Gln(Trt)-Ser(Bu^t)-Arg(Pbf)-Pro-Cys(Trt)-Val-Asp(OBu^t)-Cys(Acm)-His(Trt)-Ala-Phe-Glu(OBu^t)-Phe-Met-Gln(Trt)-Arg(Pbf)-Ala-Leu-Gln(Trt)-Asp(OBu^t)-Leu-Arg(Pbf)-Lys(Boc)-Thr(Bu^t)-Ala-Tyr(Bu^t)-Ser(Bu^t)-Leu-Asp(OBu^t)-Ala-Arg(Pbf)-Thr(Bu^t)-Glu(OBu^t)-Thr(Bu^t)-Leu-Leu-Leu-Gln(Trt)-Ala-Glu(OBu^t)-Arg(Pbf)-Arg(Pbf)-Ala-Leu-Cys(Trt)-Ala-Cys(Acm)-Trp(Boc)-Pro-Ala-Gly-Arg(Pbf)-Wang resin (130 mg). The resin (46 mg, 3.6 µmol) was treated with the TFA cocktail (TFA-TIS-DODT, 95:2.5:2.5, 1.0 mL) for 2 hours at room temperature. The reaction mixture was filtered, and the filtrate was concentrated by an N₂ stream and precipitated with ether. The precipitate was washed with ether (×5) and dried *in vacuo*. The crude peptide 14 was dissolved in 6.0 M GdnHCl aq. (1.0 mL) at room temperature, diluted with 50 mM Tris containing 0.5 M GdnHCl and 10% DMSO (36 mL, pH 8.5), then the resultant solution was stirred for 17 h at room temperature. The mixture was then acidified by the addition of 10% TFA aq. and purified by RP-HPLC to give [Cys(Acm)^{18,57}]-NICOL 15 (2.0 mg, 280 nmol, 7.8% yield). ESI MS, found: *m/z* 1755.9, 1404.8, 1171.1, calcd for [M+4H]⁴⁺: 1756.0, [M+5H]⁵⁺: 1405.0, [M+6H]⁶⁺: 1171.0, Amino acid analysis: Asp_{3,12(3)}Thr_{3,33(4)}Ser_{2,57(2)}Glu_{7,51(8)}Pro_{4,39(4)}Gly_{2,61(2)}Ala_{11,3(11)}Val_{2,09(2)}Met_{0,64(1)}Leu₇₍₇₎Tyr_{1,04(1)}Phe_{1,95(2)}His_{0,94(1)}Arg_{7,09(7)}.

NICOL 3: [Cys(Acm)^{18,57}]-NICOL 15 (69 µg, 10 nmol) was dissolved in 80% MeOH aq. (100 µL) at room temperature. I₂ (0.30 µmol, 77 µg) in MeOH (90 µL) containing 6.0 M HCl (7.0 µL) was dropwise added to the mixture and the solution was stirred

for 15 minutes at room temperature. The mixture was then quenched by the addition of ascorbic acid aq. and purified by RP-HPLC to give NICOL 3 (31 µg, 4.4 nmol, 44% yield). ESI MS, found: *m/z* 1719.7, 1376.2, 1147.5, calcd for [M+4H]⁴⁺: 1720.0, [M+5H]⁵⁺: 1376.2, [M+6H]⁶⁺: 1147.0. Amino acid analysis Asp_{3,13(3)}Thr_{3,35(4)}Ser_{2,55(3)}Glu_{7,28(8)}Pro_{4,33(4)}Gly_{2,28(2)}Ala_{11,6(11)}Val_{2,05(2)}Met_{0,20(1)}Leu₇₍₇₎Tyr_{1,04(1)}Phe_{2,08(2)}His_{1,32(1)}Arg_{7,26(7)}.

4.4. Protein Pulldown Assay

The NELL2 pulldown assay was performed as previously described.^[9,10] A total of 10 µg of the recombinant or synthetic mouse NICOL protein was conjugated to a 15 µL bed volume of NHS-activated agarose beads (Thermo Fisher Scientific, #26200) according to the manufacturer's instructions. The NICOL-conjugated beads were incubated with purified recombinant mouse NELL2 at a final concentration of 25 µg/mL in binding buffer (20 mM Tris-HCl, pH 7.4, 150 mM NaCl, 1% Triton X-100, 1% BSA) at 4 °C overnight with gentle rotation. After incubation, the beads were washed three times with 1 mL of wash buffer (20 mM Tris-HCl, pH 7.4, 150 mM NaCl, 1% Triton X-100). Each wash involved vortexing for 10 seconds followed by centrifugation at 2,000 rpm for 10 seconds, after which the supernatant was discarded. The bound proteins were then eluted in 100 µL of SDS-PAGE sample buffer. A 5 µL aliquot of the eluate or 0.3 ng of NELL2 protein was subjected to SDS-PAGE under reducing conditions, followed by immunoblotting.

4.5. Immunoblot Analyses

The proteins were separated by SDS-PAGE using e-PAGE precast gel (Atto, Japan, #E-T/R/D520L) under reducing conditions. Precision Plus Protein Dual Color Standards (Bio-Rad, #1610374) was used as a molecular weight standard. The separated proteins were electrotransferred onto polyvinylidene difluoride membranes using the TransBlot Turbo system (Bio-Rad, #1704150J). The immunoblot analyses of the transferred proteins were performed using the iBind Flex Western device (Thermo Fisher Scientific, SLF2000), iBind Flex cads (Thermo Fisher Scientific, SLF2010), and iBind solution kit (Thermo Fisher Scientific, SLF1020). The anti-NELL2 polyclonal antibody (Proteintech, #11268-1-AP) was used as the primary antibody at a final concentration of 1 µg/mL, and horseradish peroxidase-conjugated goat polyclonal anti-rabbit IgG (Jackson ImmunoResearch, #111-036-045) was used as the secondary antibody at a dilution of 1:10,000. The immunoblot signals were developed using Chemi-Lumi One Super (Nacalai Tesque, #02230) and the resulting chemiluminescent signals were captured using the Amersham ImageQuant 800 (Cytiva).

4.6. CD Spectrum Measurement

The recombinant and synthetic NICOL were dissolved in 20 mM 2-morpholinoethanesulfonic acid (MES) containing 30 mM NaCl

(pH 6.0) at concentrations of 5.0 μM (for 1), 2.9 μM (for 3) and 3.6 μM (for 4), and the CD spectra were measured between 195 and 260 nm for 16 times using a 1 mm light path length cell at 25 $^\circ\text{C}$.

4.7. Surface Plasmon Resonance Assay

SPR-based assays were conducted on Biacore 8 K (Cytiva, MA). The sensor chip NTA was activated by 0.5 mM NiCl aq. at the flow rate of 10 $\mu\text{L}\cdot\text{min}^{-1}$ for 60 s. The NELL2 was then immobilized on the chip at a flow rate of 10 $\mu\text{L}\cdot\text{min}^{-1}$ for 60 s (to \sim 500-1000 RU). NICOL was diluted to a threefold series and flowed over the chip at the flow rate of 30 $\mu\text{L}\cdot\text{min}^{-1}$ for 120 s for kinetic analysis (an empty channel was set in each group as the control). NICOL bound on the chip was dissociated by running buffer (PBS containing 0.05v/v% Tween[®]20) at the flow rate of 30 $\mu\text{L}\cdot\text{min}^{-1}$ for 600 s. Sensor Chip NTA was regenerated by EDTA aq. (350 mM, pH 7.4) at the flow rate of 30 $\mu\text{L}\cdot\text{min}^{-1}$ for 60 s. The results were analyzed on Biacore Insight Evaluation software to afford the association rate constants (k_a), dissociation rate constants (k_d) and dissociation constants (K_D).

Supporting Information

The result of MALDI-TOF MS analysis of recombinant NICOL 1, the procedure and the results of SS bond determination of SS isomer 4 and the recombinant NICOL 1.

Acknowledgments

This work was supported in part by KAKENHI grants from the Ministry of Education, Culture, Sports, Science and Technology (MEXT)/Japan Society for the Promotion of Science (JSPS) (JP25H00995, JP24H02044, JP21H02487 for D.K., JP23K23464 for H.H., and JP24K17788 for T.T.), the Japan Science and Technology Agency (JPMJPR2143), the Japan Foundation for Applied Enzymology (2023-10), the Chugai Foundation for Innovative Drug Discovery Science (2022-I-05), the Uehara Memorial Foundation, and the Mitsubishi Foundation, all to D.K. This work was also partially conducted under the Collaborative Research Program of the Institute for Protein Research, Osaka University (CR-23-01, CR-24-01, and CR-25-01), awarded to D.K. and H.H.

Conflict of Interest

The authors declare no competing interests.

Data Availability Statement

The data that support the findings of this study are available from the corresponding author upon reasonable request.

Keywords: chemical synthesis · lumicrine · NELL2 · NICOL

- [1] S. Breton, A. V. Nair, M. A. Battistone, *Andrology* **2019**, *7*, 631.
- [2] D. Kiyozumi, *Genes Cells* **2023**, *28*, 757–763.
- [3] E. R. James, D. T. Carrell, K. I. Aston, T. G. Jenkins, M. Yeste, A. Salas-Huetos, *Int. J. Mol. Sci.* **2020**, *21*, 1.
- [4] B. Robaire, B. T. Hinton, "The epididymis" in *Knobil and Neill's Physiology of Reproduction*, Elsevier, **2015**, pp. 691–771.
- [5] K. A. Moniem, T. D. Glover, C. W. Lubicz-Nawrocki, *J Reprod Fertil* **1978**, *54*, 173.
- [6] D. W. Fawcett, A. P. Hoffer, *Biol. Reprod.* **1979**, *20*, 162.
- [7] D. Kiyozumi, T. Noda, R. Yamaguchi, T. Tobita, T. Matsumura, K. Shimada, M. Kodani, T. Kohda, Y. Fujihara, M. Ozawa, Z. Yu, G. Miklossy, K. M. Bohren, M. Horie, M. Okabe, M. M. Matzuk, M. Ikawa, *Science* **2020**, *368*, 1132.
- [8] B. T. Hinton, Z. J. Lan, D. B. Rudolph, J. C. Labus, R. J. Lye, *J Reprod Fertil Suppl.* **1998**, *53*, 47–57.
- [9] D. Kiyozumi, K. Shimada, M. Chalick, C. Emori, M. Kodani, S. Oura, T. Noda, T. Endo, M. M. Matzuk, D. H. Wreschner, M. Ikawa, *Nat. Commun.* **2023**, *14*, 2354.
- [10] D. Kiyozumi, *Reprod Biol Endocrinol* **2024**, *22*, 3.
- [11] D. Kiyozumi, N. Sugimoto, K. Sekiguchi, *Proc Natl Acad Sci U S A* **2006**, *103*, 11981.
- [12] R. Manabe, K. Tsutsui, T. Yamada, M. Kimura, I. Nakano, C. Shimono, N. Sanzen, Y. Furutani, T. Fukuda, Y. Oguri, K. Shimamoto, D. Kiyozumi, Y. Sato, Y. Sado, H. Senoo, S. Yamashina, S. Fukuda, J. Kawai, N. Sugiura, K. Kimata, Y. Hayashizaki, K. Sekiguchi, *Proc Natl Acad Sci U S A* **2008**, *105*, 12849.
- [13] T. J. Carney, N. M. Feitosa, C. Sonntag, K. Slanchev, J. Kluger, D. Kiyozumi, J. M. Gebauer, J. Coffin Talbot, C. B. Kimmel, K. Sekiguchi, R. Wagener, H. Schwarz, P. W. Ingham, M. Hammerschmidt, *PLoS Genet.* **2010**, *6*, e1000907.
- [14] D. Kiyozumi, M. Takeichi, I. Nakano, Y. Sato, T. Fukuda, K. Sekiguchi, *J. Cell Biol.* **2012**, *197*, 677.
- [15] R. Sato-Nishiuchi, I. Nakano, A. Ozawa, Y. Sato, M. Takeichi, D. Kiyozumi, K. Yamazaki, T. Yasunaga, S. Futaki, K. Sekiguchi, *J. Biol. Chem.* **2012**, *287*, 25615.
- [16] S.-J. Jeong, R. Luo, K. Singer, S. Giera, J. Kreidberg, D. Kiyozumi, C. Shimono, K. Sekiguchi, X. Piao, *PLoS One* **2013**, *8*, e68781.
- [17] Y. Sato, D. Kiyozumi, S. Futaki, I. Nakano, C. Shimono, N. Kaneko, M. Ikawa, M. Okabe, K. Sawamoto, K. Sekiguchi, *Mol. Biol. Cell* **2019**, *30*, 56–68.
- [18] D. Kiyozumi, Y. Taniguchi, I. Nakano, J. Toga, E. Yagi, H. Hasuwa, M. Ikawa, K. Sekiguchi, *Life Sci Alliance* **2018**, *1*, e201800064.
- [19] D. Kiyozumi, I. Nakano, R. Sato-Nishiuchi, S. Tanaka, K. Sekiguchi, *Life Sci. Alliance* **2020**, *3*, e201900515.
- [20] R. B. Merrifield, *J. Am. Chem. Soc.* **1963**, *85*, 2149.
- [21] J. Wu, J. T. Watson, *Protein Sci.* **1997**, *6*, 391.
- [22] S. Nakagawa, Y. Tamakashi, T. Hamana, M. Kawase, S. Taketomi, Y. Ishibashi, O. Nishimura, T. Fukuda, *J. Am. Chem. Soc.* **1994**, *116*, 5513.

Manuscript received: April 30, 2025

Revised manuscript received: July 4, 2025

Version of record online: July 26, 2025